



RESTRAINED FLEXURE OF BRITTLE-MATRIX COMPOSITE STRUCTURES

M. J A N A S and J. S O K Ó Ł - S U P E Ł

**POLISH ACADEMY OF SCIENCES
INSTITUTE OF FUNDAMENTAL TECHNOLOGICAL RESEARCH**

ul. Świętokrzyska 21, 00-049 Warsaw, Poland

Restrained flexure analysis concerns transversal bending of flat structures with in-plane displacements at supports prohibited or restricted. If the material characteristics are different in tension and in compression, these restraints generate important membrane forces (the arching action effect). It strengthens considerably the structure, but renders its response strongly nonlinear and unstable. In a recent introductory study the authors concluded that their old approximate analytical approach to restrained flexure of elastic-plastic beams and slabs gives qualitatively good results and may be useful to replace cumbersome numerical procedures. Here, a parametric study using an incremental FEM analysis is performed enabling the determination of input data needed for an elementary but reliable approximate approach. Different load and support configurations for beam systems are considered and the structure sensitivity to support compliance is studied. Numerical and approximate analytical results are compared with results of a series of collapse tests on elastically restrained RC beams.

1. RESTRAINED FLEXURE

When supports of the structure enable transmission of stress resultant components parallel to the reference plane of a flat structure, the simple bending response to transversal loads (ensuring the absence of membrane stress resultants) may occur only in a very particular situation. The latter needs that the flexural behavior in the dynamical and in the kinematical sense coincide. In the case of clamped beams or slabs, the above may appear only in structures built of a material with the same strength and elasticity characteristics in tension and in compression ("symmetric" material). In this situation, even if the membrane forces appear (at large deflections or due to very particular support conditions), they will be of a rather secondary importance for the overall structure response.

If the material characteristics differ in tension and compression, membrane forces will appear, generated by the support restrictions, even if the applied load

is exclusively transversal. This case will be called restrained flexure, *per analogiam* to restrained torsion. For “non-symmetric” materials, when the compressive strength is superior to the tensile strength, the restrained flexure is accompanied by important compressive membrane forces (the “arching action” effect). They appear already from the very beginning of the loading process and may considerably strengthen the structure, both in its initial rigidity and, especially, in its ultimate load-carrying capacity.

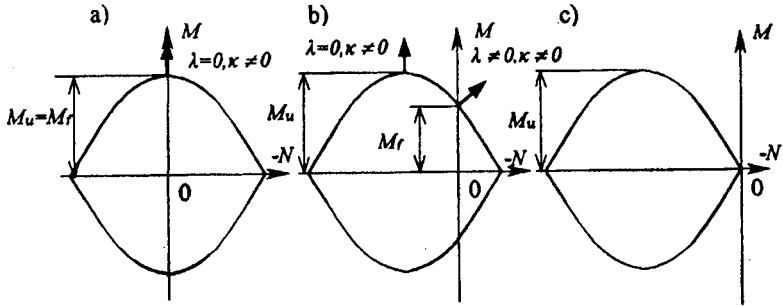


FIG. 1. Yield curves for a uniform cross-section of a one-way slab: a) symmetric material, b) non-symmetric material, c) no-tension material.

The above may be illustrated using the simplest example: plastic yielding of a uniform cross-section of a one-way slab. The corresponding yield curves are shown in Fig. 1. If the yield stresses in compression and in tension are the same, we have, following the associated plastic flow rule, simultaneous absence of the mid-plane deformation rates ($\lambda = 0$) and of membrane forces ($N = 0$), Fig. 1a. However, if the yield stresses are different, this coincidence disappears (Fig. 1b). At $N = 0$ the flow vector $\mathbf{v}(\kappa, \lambda)$, normal to the curve, has two non-vanishing components (curvature rate κ and the mid-plane deformation rate λ). The curves in Fig. 1 correspond to the mid-plane of the cross-section chosen as the reference axis. Of course, the simultaneous absence of the two in-plane variables ($\lambda = 0, N = 0$) may be obtained if the reference axis coincides with the local neutral axis. However, this coincidence appear either at positive or at negative bending, because the axis position is in both cases different. Therefore, a pure flexural behavior should mean either $N = 0$ (with the flexural strength of the cross-section $M = M_f$) or $\lambda = 0$ (with its ultimate strength $M = M_u$). These values may be strongly different ($M_u \gg M_f$) and, in the case of a no-tension material (Fig. 1c), the structure having no strength in simple bending ($M_f = 0$) may be significantly resistant under the conditions of restrained flexure, when in-plane displacements at supports are prohibited ($M = M_u$). The arching effect was mentioned already long ago [1] and was even taken into account (in an empirical manner) in certain old structural codes, e.g. [2].

Neglecting the insight into the conditions necessary for the simple bending response may provoke some confusion, namely in the analysis of concrete structures. For example, the effect of restrained flexure appearing in reinforced concrete plates is responsible for the so-called yield-line paradox. The yield line method used in the limit analysis of reinforced concrete plates should give upper bounds to their load-carrying capacities. However, the results obtained by this method are frequently inferior to experimental data. It appears [3] that yield-line deformation patterns corresponding to simple flexural situations, but including both the positive and negative bending, may appear kinematically inadmissible, when they are associated with pure flexural yield moments M_f . On the other hand, if M_f were replaced by the ultimate moment M_u compatible with a purely flexural deformation pattern, the approach would become kinematically admissible but would give excessively high limit load estimates.

This strengthening effect is well known to structural engineers as the “dome effect” (or arching action) in built-in reinforced concrete slabs, e. g. [4]. If the supports are able to withstand important membrane forces due to restrained flexure conditions, the structure can support loads considerably exceeding their flexural carrying capacities. However, the loading process ends in this case with an abrupt dynamic breakdown. Because of this unstable behavior and its sensitivity to secondary factors, such as initial imperfections or support tolerances, the effect is rarely taken into account in assessments of the structural safety, this fact resulting frequently in a very conservative design.

2. ULTIMATE-LOAD ANALYSIS BY A POST-YIELD APPROACH (PYA)

Flexural behavior being strongly nonlinear, when accompanied by important compressive membrane forces, the problem needs a large-displacement approach even at very small deflections. Therefore, in these situations the classical limit analysis approach cannot be satisfactory for determination of the load-carrying capacities of the structures. To take into consideration the configuration changes, a post-yield approach (PYA) was applied already long ago [5, 4]. It consists of applying the kinematical method of the limit analysis theory to structures with their geometry modified following a plastic collapse mode. This mode may correspond to the initial plastic flow or may be updated during the deformation process. In this way, a load-deformation curve may be obtained corresponding to a sequence of instantaneous collapse loads for a consecutively deformed structure. In the Fig. 2 instantaneous collapse modes are shown for deformed one-way (strips) and two-way slabs.

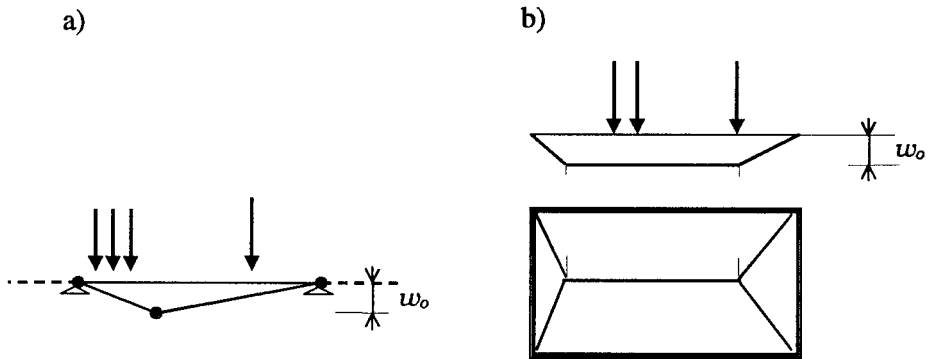


FIG. 2. Collapse modes for (a) one-way and (b) two-way slabs at large deflections.

The post-yield approach has been applied, first of all, to one-way or two-way concrete slabs using relations inherent to the deformation theory of plasticity, e.g. [6, 7, 8] or to the flow theory, e.g. [9, 10, 11]. When concerning applications to the kinematical approach using yield-line (plastic hinge) patterns, this difference concerns only the assumption on the sign of the stress normal to the yield-line. It depends either upon the sign of the corresponding plastic strain (in the deformation theory) or on the sign of the strain rate (in the flow theory). If the incipient collapse is concerned, the two theories give the same result. However, that is not the case, when a deformed configuration is considered. In the case of ductile (“symmetric” or “non-symmetric”) materials, the correct approach should be based, of course, on the flow theory. In the case of perfect no-tension materials (unilateral contact), the deformation theory is pertinent [12] at tension-to-compression strain reversals but it is not so at compression-to-tension reversals. For brittle materials an intermediate approach may be justified. Therefore, proper choice of the theory is not obvious. If the flow theory is used in an elastic-plastic PYA analysis [13] it leads to a differential form of the kinematical compatibility relations. This form enables a proper choice of initial conditions for membrane forces. Hence, a qualitatively correct description of the structure response (an ascending-descending load deflection curve) and determination of the ultimate supportable peak-load become possible. On the other hand, when the deformation theory is used, compatibility rules inherent to the limit analysis theory cannot be strictly followed. Therefore, the flow approach seems to be more convenient and is assumed here as a basis for an approximate approach, even if it does not follow the real constitutive rules at certain strain reversals. This choice seems to be right, as confirmed by a complete incremental FEM analysis [14].

Since the limit analysis theory furnishes instantaneous load-carrying capacities for a given fixed geometrical configuration, it cannot determine the prior-to-collapse deformations. Unfortunately, these deformations are of primary im-

portance in the restrained nonlinear bending. The limit analysis theory, when applied to the rigid-plastic model of the deformed structure, gives a descending load-deflection curve, Fig. 3. The maximum supportable load, obtained in this way, appears at incipient collapse and its value strongly overestimates the structure carrying capacity. If elastic prior-to-collapse deformations were tried to be accounted for, the main advantage of the limit analysis approach – its simplicity – would be lost. Fortunately, it appears that elastic flexural deformations have only a limited (quantitative) influence on the structure behavior, whereas they are responsible for the computational complexity of the analysis. On the other hand, elastic deformations due to membrane forces are responsible for qualitative changes in the structural response. Taking into account the elastic membrane compliance and neglecting flexural deformations outside the yield lines allows for an approach [13] that describes qualitatively correctly the structure behavior, when conserving the simplicity of the post-yield analysis. However, the membrane compliance of elastic links between the yield lines and the compliance of the supports has to be replaced by a kind of spring action. A reduced average compliance of these springs has to be properly chosen [14]. This problem will be discussed later on the basis of numerical FEM analysis.

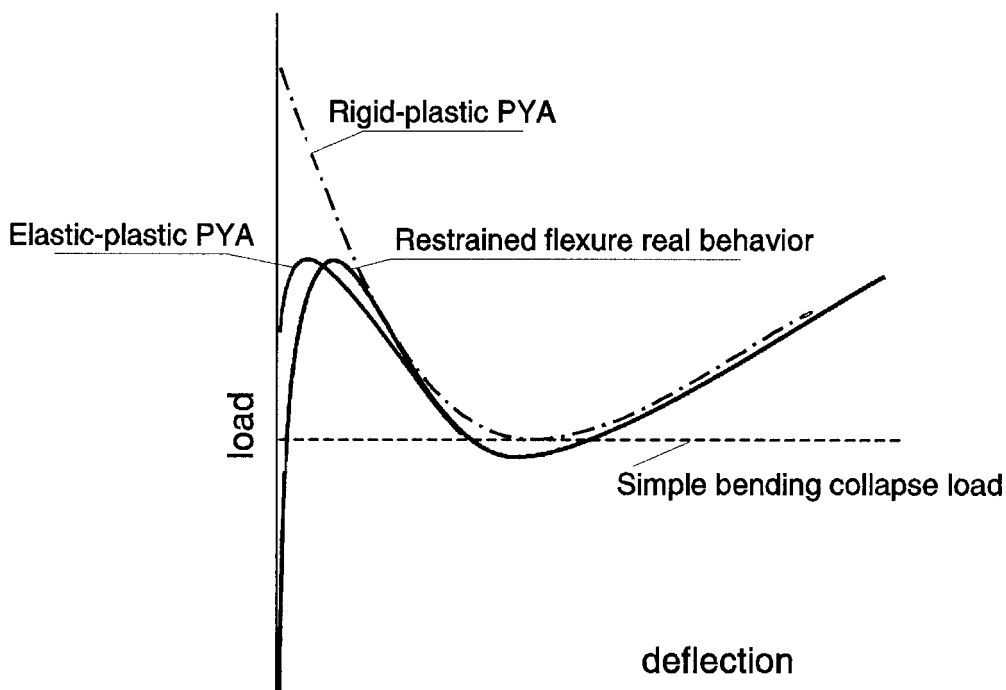


FIG. 3. Load-deflection response in restrained flexure and its post-yield approximations.

Let us recall the idea of this approach, when considering a classical case of a strip deformed following a three-hinge mode, Fig. 2a. If a virtual rotation increment $d\theta$ is acting on the rigid-plastic strip (Fig. 4), kinematical compatibility needs the vectors of relative rotation increments in the plastic hinges (yield-lines) to be co-planar. In the case of the same reinforcement at both supports, chosen here for simplicity of the demonstration, it means that this plane (instantaneous neutral plane) is parallel to the reference plane of the undeformed structure. Hence, the positions of instantaneous neutral axes z (Fig. 4) in the yield lines satisfy a relation: $z_p = z_n - w$. However, if the strip is assumed to submit elastic membrane deformations proportional to the membrane force increment dN , this relation becomes:

$$(2.1) \quad z_p = z_n - w - \frac{dN}{dw} \frac{l_l l_r}{Eh}.$$

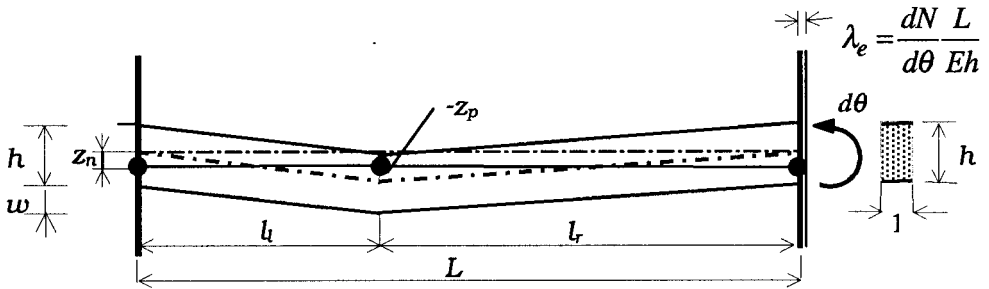


FIG. 4. Kinematics of an instantaneous flow of the deformed strip, following an incipient collapse mode.

In a non-dimensional form compatible with [13, 14] this relation may be rewritten as follows:

$$(2.1)' \quad \xi_p = \xi_n - 2\alpha - \frac{2}{\varepsilon} \frac{dn}{d\alpha}$$

Notation in the above formulas is as follows: ξ_n, ξ_p describe positions of neutral axes: $\xi_i = 2 z_i : h$ (subscripts $i = n, p$ concern negative-support and positive-span yield lines, respectively); l_l, l_r describe the position of the positive yield line (Fig. 4); $L = (l_l + l_r)$ is the strip span and h - its thickness; E, R - are, respectively, Young's modulus and plastic yield stress of the matrix material; α is the non-dimensional reference deflection: $\alpha = w : h$; n is a non-dimensional membrane force: $n = 2N : (Rh)$, compression being taken positive.

The elastic stiffness parameter ε is

$$(2.2) \quad \varepsilon = \frac{2Eh^2}{Rl_r l_l}.$$

The positions of instantaneous neutral axes in the yield-lines ($z = \lambda : \kappa$) describe, through the normality rule (Fig. 1), the values of the stress resultants there. The membrane forces may be determined using known expressions for the yield curves, e.g. [13], and then, the compatibility relation (2.1) may be presented in terms of these forces. Moreover, equilibrium needs the membrane forces in the plastic cross-sections to be equal, if horizontal external loads are absent and if displacements are small as compared to the structure span. This condition, together with the relation (2.1), results in a linear differential equation for the membrane force in function of the deflection w . This equation, with the initial condition for the deformation process ($N = 0$ at $w = 0$), describes the evolution of the non-dimensional membrane force:

$$(2.3) \quad n = (1 - e^{-\varepsilon\alpha}) \left(k + \frac{1}{\varepsilon} \right) - \alpha,$$

where k depends on the plastic properties of the cross-sections. For unreinforced or symmetrically face-reinforced cross-sections with a no-tension matrix we have $k = 1$ (see [13]). Then, the positions of instantaneous neutral axes in the cross-sections ξ_n, ξ_p may be also determined and, hence, the yield moments M_p, M_n in positive and negative bending may be found.

Limit equilibrium of the structure shown in Fig. 1 is written as:

$$(2.4) \quad M_{load} = M_p - M_n - Nw,$$

where M_{load} is the maximum bending moment from the transversal load determined as for a simply supported strip. Introducing (2.3) to the Eq. (2.4), together with the expressions for ξ_n, ξ_p easily found from the yield criterion (e.g. [13]) when n is already known, we obtain finally the load-deflection relation [13], which may be written in a non-dimensional form:

$$(2.5) \quad q = \frac{M_{load}}{2M_0} = q_Y + (k - \alpha^2) - \left[k - (1 - e^{-\alpha\varepsilon}) \left(k + \frac{1}{\varepsilon} \right) \right]^2.$$

Here q_Y is the collapse load in unrestrained bending of the undeformed structure, and M_0 – the ultimate moment of the unreinforced cross-section $M_0 = (Rh^2 : 8)$ corresponding to M_u in Fig. 1c.

It appears that for symmetrically loaded structures, the ultimate load q_U occurs at the central deflection α_U being one half of the value corresponding to the maximum of the axial force, i.e.:

$$(2.6) \quad \alpha_U = \frac{\ln(1 + k\varepsilon)}{2\varepsilon},$$

and can be expressed by a formula:

$$(2.7) \quad q_U = q_Y + \varepsilon^{-2} \left[\left(k\varepsilon - \ln \sqrt{1 + k\varepsilon} \right)^2 - \left(\sqrt{1 + k\varepsilon} - 1 \right)^2 \right].$$

3. INCREMENTAL VS. THE POST-YIELD APPROACH

Geometrical non-linearity of the structure behavior under restrained bending conditions is enhanced by the fact that the membrane forces are self-generated by the deformation process. Therefore, the simulation of the response, even in the simplest quasi-static case, may pose serious numerical problems. Of course, it may be performed using a FEM approach (even by commercial FEM codes). However, the corresponding incremental procedures are rather cumbersome and, first of all, very sensitive to modifications of boundary and initial conditions. Therefore, a reliable simulation of the unstable response furnishing the value of the supportable peak-load capacity of the structure needs very precise input data. Uncertainties concerning some features of these conditions and data make engineers reluctant in accounting for the arching action and, hence, important strength reserve of the structure may be neglected. The above conclusion has motivated studies concerning a possible implementation of the approximate approach into practical structural analysis and diagnostics.

In the former paper [14] the authors used an incremental FEM analysis by ABAQUS code [15] to verify the reliability of the post-yield approach. Elastic-perfectly plastic material model is assumed: no-tension for the matrix and “symmetric” ductile for the reinforcement layers. The study concluded in a qualitatively good correlation of its results with the post-yield approach in the case of a centrally loaded strip. However, a larger set of load configurations, support conditions and material characteristics should be considered to make sure that the coincidence does not concern only some particular cases.

The first problem that could make the approximate approach to be of limited utility for practical purposes concerns similarity requirements. The real load-deflection relation, obtained from the incremental FEM analysis, depends upon numerous geometric and strength parameters. In the corresponding approximate relation (2.5) all these parameters enter to one resulting parameter – the stiffness ratio ε . It is obvious (e. g., from simple considerations of reinforced elastic structures) that incremental analysis would give non-identical results for the same value of the parameter ε , if its components are modified. On the other hand, in all these cases the approximate solution (2.5) will be the same. The corresponding parametric study has shown that the differences concern first of all the ascending parts of the load-deflection curve: the initial elastic phase and the near-to-membrane behavior at very large displacements. Both these phases are of minor interest for the evaluation of the structure strength. As may be shown on the example of simultaneously varying slenderness ratio $\Lambda = L : h$ and the compressive Young modulus of the matrix material E_c , when the parameter ε remains constant (Fig. 5), the curves from the incremental (“exact”) analysis are

very similar in the vicinity of the supportable ultimate-peak load of the structure. For unreinforced no-tension matrix the curves in the up-to-collapse phase are practically identical. Reinforcement makes this coincidence impossible in the initial phase. However, even for very high reinforcement ratios

$$(3.1) \quad \eta = \frac{\sigma_s A_s}{Rh},$$

(σ_s and A_s mean, respectively, the yield stress and the thickness of the ductile reinforcement layer) the coincidence is satisfactory, when concerning the ultimate-peak load zone. Similar conclusions concern modification of other parameters with ε remaining constant.

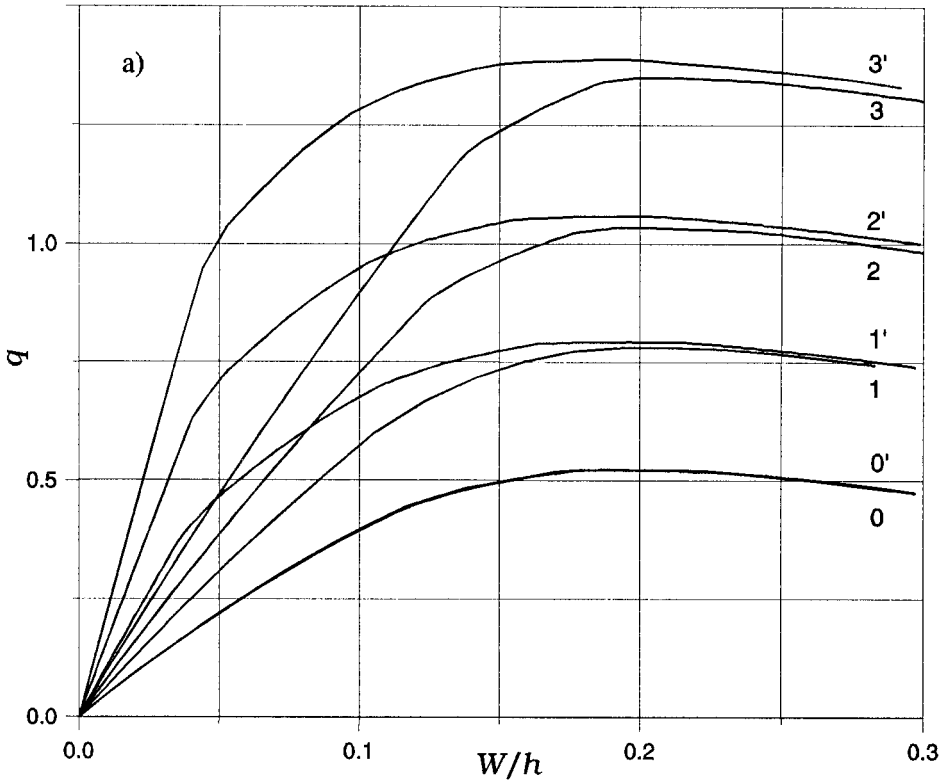


FIG. 5. Similarity of the load-deflection relations (FEM incremental analysis) for a constant elastic stiffness ratio $\varepsilon = \text{const.} = 60$, with its components: slenderness ratio $\Lambda = L : h$ and Young modulus E varying simultaneously. Symmetrically face-reinforced strips with different reinforcement intensity: $\eta = 0$, $\eta = 0.031$, $\eta = 0.062$, $\eta = 0.10$ (curves 0, 1, 2, 3, respectively), with the slenderness ratio $\Lambda = L : h = 7$ and $E = 15$ Gpa. The curves 0', 1', 2', 3' correspond to $\Lambda = 14$ and $E = 60$ Gpa. a) up-to-ultimate load phase.

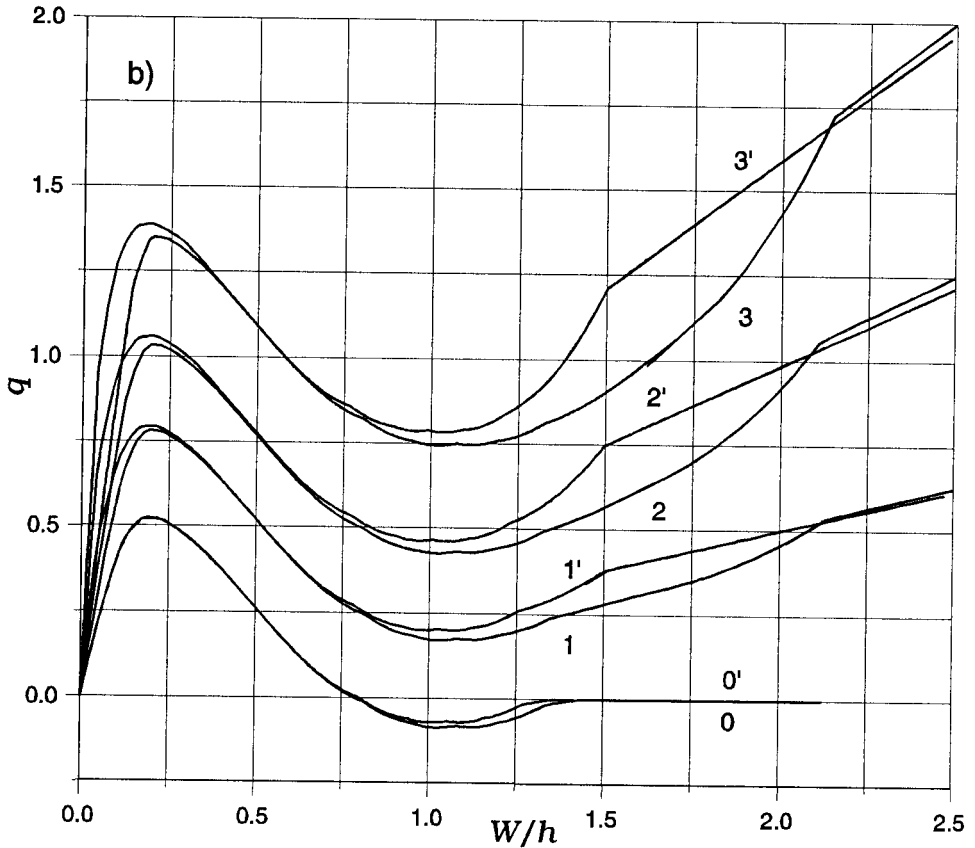


FIG. 5. Similarity of the load-deflection relations (FEM incremental analysis) for a constant elastic stiffness ratio $\epsilon = \text{const.} = 60$, with its components: slenderness ratio $\Lambda = L : h$ and Young modulus E varying simultaneously. Symmetrically face-reinforced strips with different reinforcement intensity: $\eta = 0$, $\eta = 0.031$, $\eta = 0.062$, $\eta = 0.10$ (curves 0, 1, 2, 3, respectively), with the slenderness ratio $\Lambda = L : h = 7$ and $E = 15$ Gpa. The curves 0', 1', 2', 3' correspond to $\Lambda = 14$ and $E = 60$ Gpa. b) entire load-deflection curves.

The above permits to exclude doubts concerning the similarity problems that would disqualify the approximate approach. Therefore, since the final expression for the ultimate load (2.7) may be accepted if the ratio ϵ is properly reduced to give reliable results, this may be obtained by a reduction of the Young modulus of the matrix. The introductory study [14] indicated that the best fit of the ultimate-peak loads from both approaches is ensured if the Young modulus introduced into the ratio ϵ is reduced by 2. A slightly better fit is obtained if this reduction is smaller, depending upon the reinforcement ratio. Such improvement is taken into account and discussed later in Fig. 8. However, that produces, in fact, the ratio ϵ dependent upon the reinforcement characteristics and reduces simplicity of the

approach. Taking into account all the simplifying assumptions (perfect plasticity, linear elasticity, etc.) inherent to both approaches, it seems that reduction of the Young modulus by half may be considered satisfactory for practical purposes. The above is illustrated in Fig. 6, using FEM curves, with the analytical ultimate-peak loads (2.7) shown by dots.

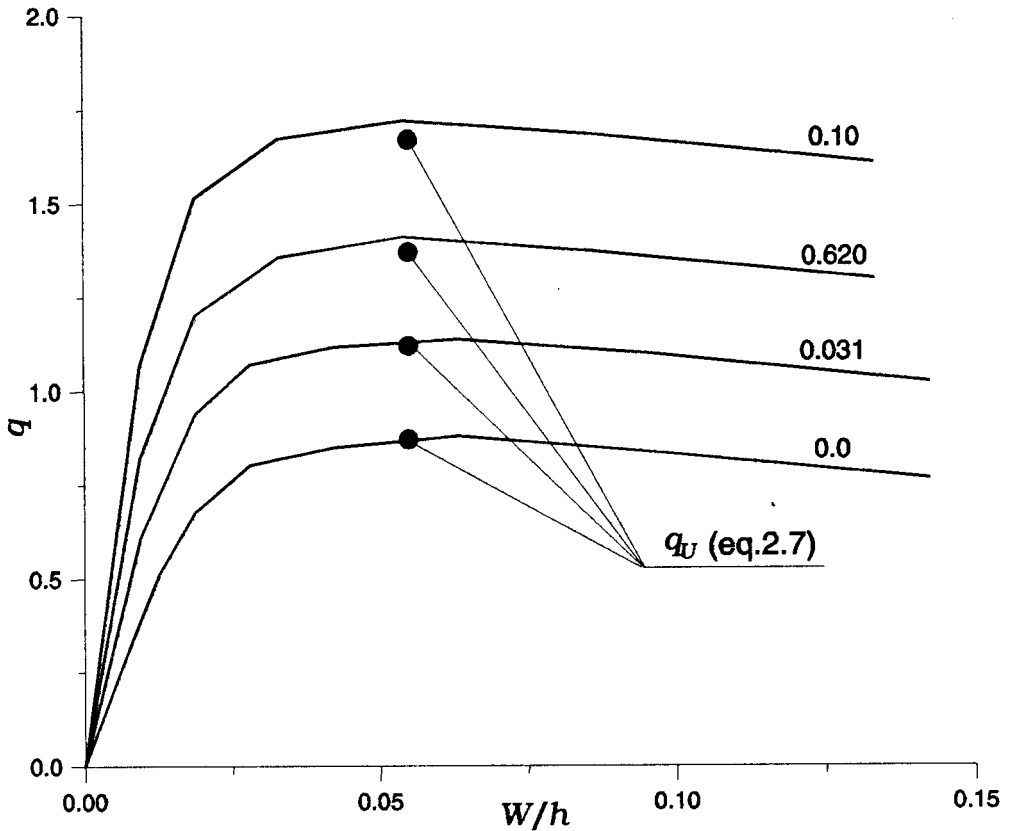


FIG. 6. Ultimate-peak loads following the incremental analysis ($\Lambda = L : h = 10, \epsilon = 60$), with different reinforcement intensities ($\eta = 0, \eta = 0.031, \eta = 0.062, \eta = 0.10$) and their analytical approximations (black dots).

4. COMPLIANT SUPPORTS

Reduction of the ultimate supportable load, due to the compressibility of the structure under membrane forces may be strongly amplified, if the supports are also compliant. For perfectly compliant supports we arrive, of course, to the simple bending conditions. The support compliance enters the approximate

solution in the same manner as the elastic deformability of the structure. The resulting stiffness ratio ε_r is determined by addition of the two compliances and, therefore, we have:

$$(4.1) \quad \frac{1}{\varepsilon_r} = \frac{1}{\varepsilon} + \frac{1}{\varepsilon_s}$$

with ε_s standing for the stiffness ratio representing both supports. To make more comprehensive the estimation of the importance of the support compliance, the load-deflection curves are given in Fig. 7 and Fig. 8 for selected ratios of the nominal membrane compliance of the strip $C = L/Eh$ and a cumulated compliance of both supports C_s . The FEM incremental and approximate PYA curves are compared there for unreinforced and bottom-face reinforced moderate-slenderness strips. The PYA curves correspond to reduction factors for the Young modulus:

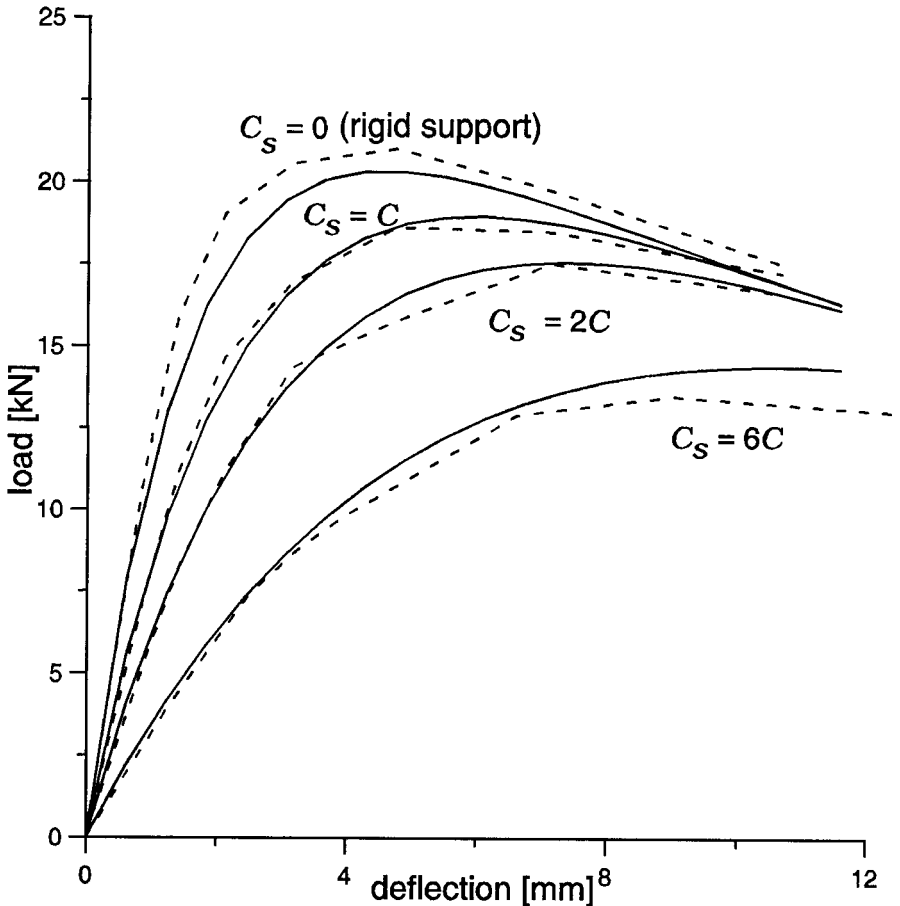


FIG. 7. Load-deflection curves for unreinforced strip with different support compliances; incremental and PYA analyses (dashed and solid lines, respectively).

$E' = E : 2$ (dashed curves) and $E' = (1 + 8\eta_m)E : 2$, with η_m standing for the mean tensile reinforcement intensity in positive and negative hinges (dotted curves). It appears that the conclusions obtained for undeformable supports are valid also for compliant supports.

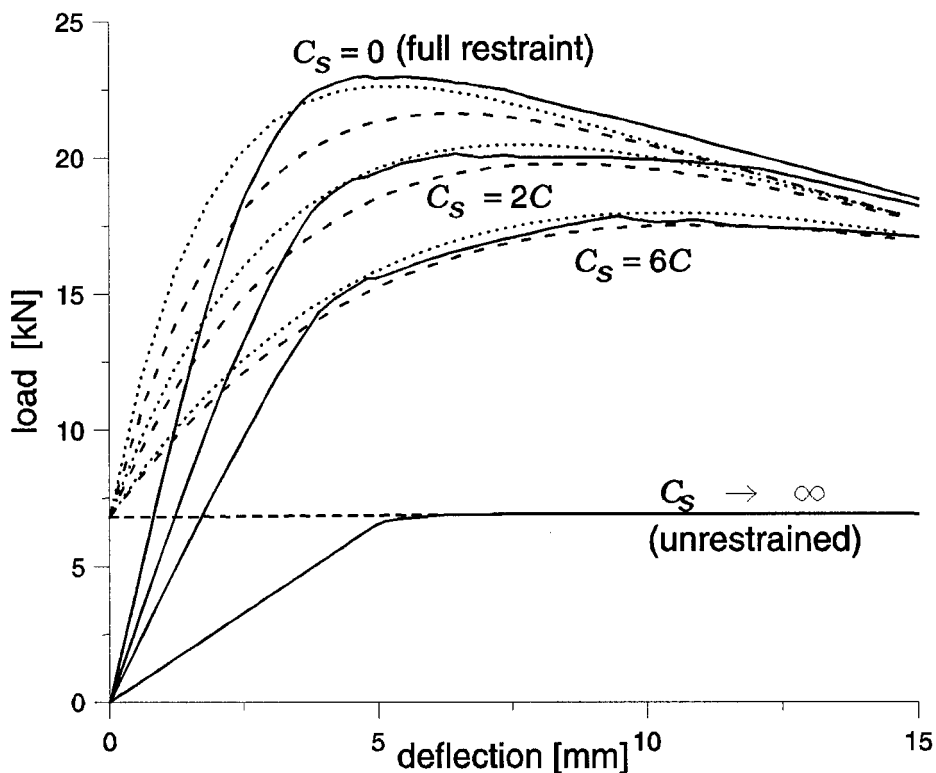


FIG. 8. Load-deflection curves for strips with a one-layer reinforcement ($\eta = 0,09$) and different support compliances. Solid curves - incremental analysis; dashed and dotted curves - approximation by the PYA approach (two reduction factors for the Young modulus).

If the supports compliance is less than one-third of the strip compliance, the supports may be considered as practically rigid. This conclusion may be of a practical importance, because in majority of practical cases, the strip supports are massive walls that may be considered as elastic half-spaces. If such a half-space is loaded by a pressure exerted by the plastic compression zone at the support yield line (Fig. 9), the classical elastic solution gives the support compliance equal from 7% to 20% of the strip compliance ($C_s = [0,07 \div 0,20]C$), depending upon the width of the strip. It means that, if a perfect initial fit is insured between a strip and a wall made of the same material, the supports may be considered undeformable. Such situations may appear e.g. in rock roofs of mining galleries.

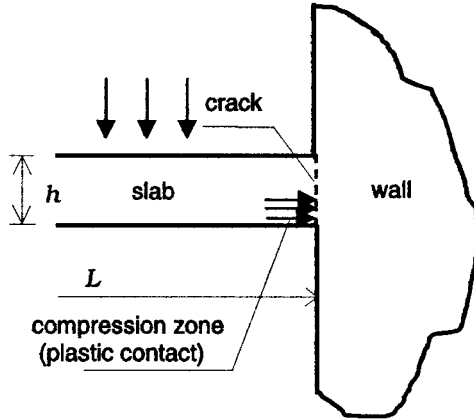


FIG. 9. Arching action in a wall-strip interaction.

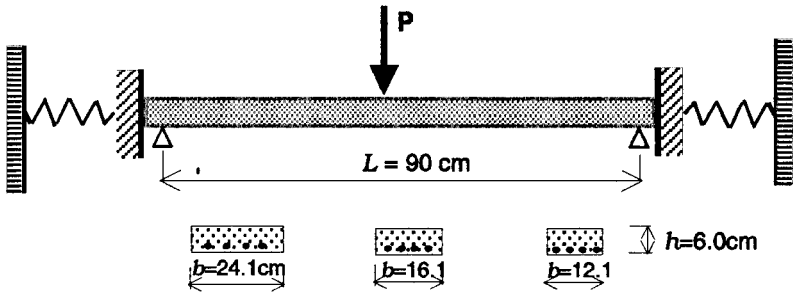


FIG. 10. Reinforced concrete strips used in the experimental program.

The results of both approximate and FEM analyses have been compared with results of a series of tests on reinforced concrete strips with elastically compliant supports in conditions of unilateral contact. The tests were a by-product of an old experimental program concerning implementation of the limit analysis theory into the design of RC plates [16]. Singly (bottom- or top-) reinforced strips were simply supported (Fig. 10) and subjected to the three-point loading tests. Different reinforcement intensities, from $\eta = 0.09$ to $\eta = 0.18$, were obtained using the same reinforcement but varying the strip width. Variable support compliance was obtained using different diameters of restraining ties (Fig. 11).

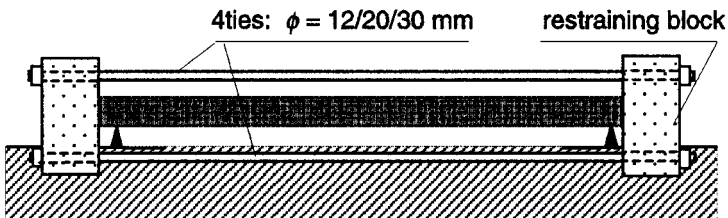


FIG. 11. Testing device for restrained bending with compliant supports.

The principal goal of the tests was visualisation of the importance of the arching action effect. Some results are shown in the Fig. 12. The restraints induced a very important rise in the collapse load in comparison with unrestrained bending: from 53% (for strong reinforcement of $\eta = 0,18$) to 171% (for $\eta = 0.09$). Of course the impact of the restraints is the most important in the case of unreinforced structures. For inverse bending (reinforcement layer close to the upper face), the collapse load attained 80% of the value obtained in normal bending (reinforcement near the lower face), whereas in the unrestrained upward bending this value was only about 20% of the structure strength in downward bending. The last observation may contribute to the discussion on the validity of the opinion on negligible importance of compressed reinforcement in brittle matrix composite structures.

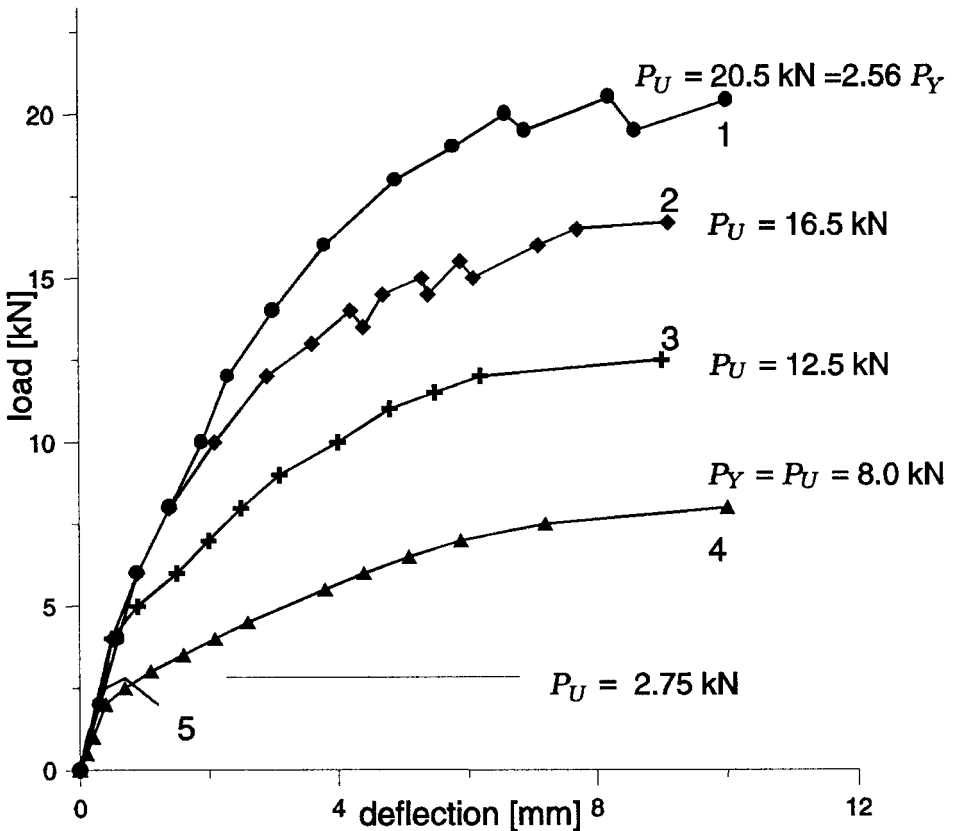


FIG. 12. Selected results from three-point restrained bending tests of RC strips 1 - reinforcement ratio $\eta = 0.09$, strongly restrained ($C_S = 2C$); 2 - unreinforced $\eta = 0$, ($C_S = 2C$); 3 - $\eta = 0$, weakly restrained ($C_S = 6C$); 4 - $\eta = 0.09$, unrestrained ($C_S \rightarrow \alpha$); 5 - $\eta = 0$, unrestrained.

The test results for different support compliances (two specimens for each case) are compared in (Fig. 13) with the curves from the incremental FEM analysis. The comparison shows a satisfactory fit of the curves. This conclusion, together with the comparison of the approximate and incremental results (Fig. 8) confirms that the approximate approach is applicable also in the structural situations considered in this section. The results (analytical) in the Fig. 13 were obtained using the concrete modulus E_c measured in the tests as a secant value at a relatively important elastic deformation. It was only 57% of the initial modulus value recommended by structural codes. Another idealisation introduced into the analysis by the model – perfect plasticity neglecting the concrete crushing/softening – does not seem to rise serious doubts. However, for practical conclusions a further study of this problem is necessary.

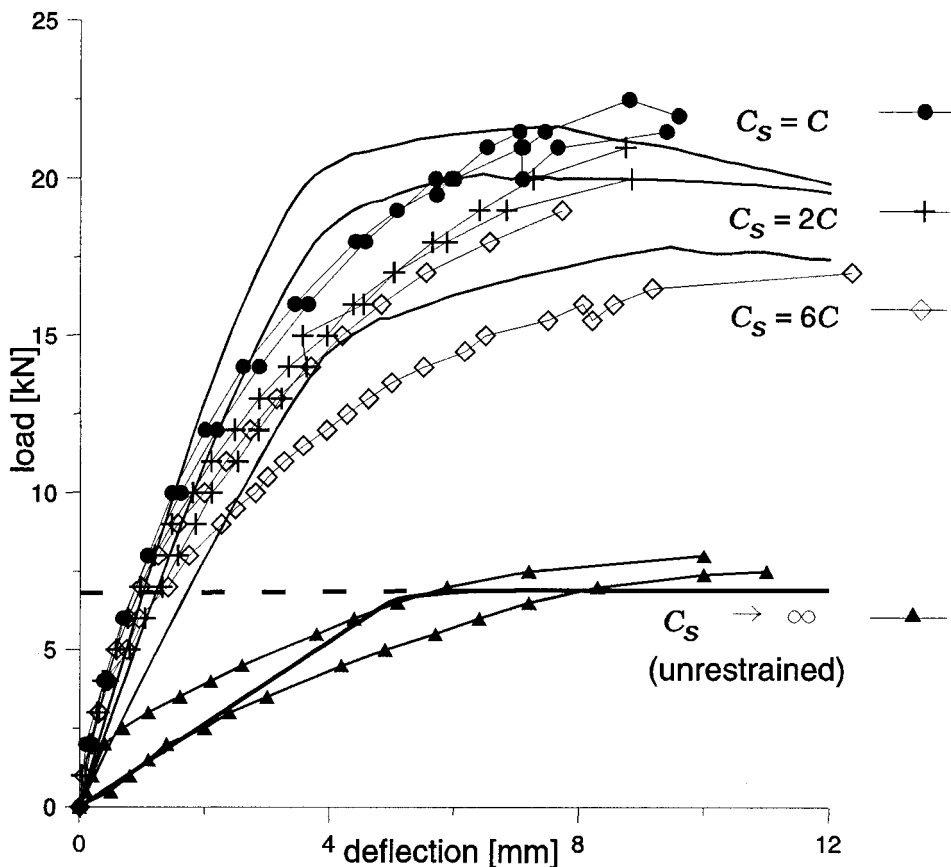


FIG. 13. Comparison of experimental load-deflection curves (lines with symbols: two tests for each compliance value: $C_S = C$ – dots, $C_S = 2C$ – crosses, $C_S = 6C$ – diamonds, $C_S \rightarrow \infty$ – triangles) with the results of the incremental FEM analysis (continuous lines) for bottom reinforced ($\eta = 0.09$) RC strips.

5. FINAL REMARKS

The parametric study of the proposed approximate analytical approach [14] to restrained bending, based on the post-yield methodology comparing it to the FEM incremental analysis, has confirmed utility of this approach to the analysis of one-way one-span slabs. Some further verification for multi-span systems and, first of all, for two-way slabs is still necessary.

To permit simple application of this approximate approach to any case of load and support configuration, a reduced value of the stiffness parameter ε should be provided from the comparative incremental analysis for some benchmark cases. This may be considered as practically achieved now. Moreover, to determine the supportable ultimate-peak load of the structure, only data from the simple rigid-plastic limit analysis are needed, concerning unrestrained bending and, of course, also yield characteristics of the reinforced cross-sections. The above needs no more than elementary knowledge of structural mechanics of the strength-of-materials level. However, the limit analysis approach, in spite of its simplicity, is not largely implemented into structural analysis and design. Therefore, for practical implementation the needed data should be given in a ready-to-use form. This task is not too challenging but useful and should be done.

For materials (like concrete) without a clear linear elastic behavior, a reduced "secant" modulus should be used. As concerns a direct application of the method to unreinforced or weakly reinforced concrete structures, incremental analysis accounting for the softening of the material is needed. It can provide, eventually, supplementary reduction factors due to crushing of the material that may occur, in some situations, earlier than the ultimate-peak load is attained.

REFERENCES

1. A.A. GVOZDEV, *The basis for the paragraph 33 of the reinforced concrete design code* (in Russian), *Stroitel'naya Promyshlennost*, **17**, 3, 51–58, 1939.
2. *Instruction for the Design of Reinforced Concrete Hyperstatic Structures Undergoing Stress redistribution* (in Russian), Gosstroyizdat, Moscow 1961.
3. M. JANAS, *Kinematical compatibility problems in yield-line theory*, *Mag.Concrete Res.*, **19**, 33–44, 1967.
4. R.H. WOOD, *Plastic and elastic design of plates*, Thames and Hudson, London 1961.
5. R.M. HAYTHORNTHWAITE, *Beams with full end fixity*, *Engineering*, **183**, 110–112, 1957.
6. K.P. CHRISTIANSEN, *The effect of membrane stresses on the ultimate strength of the interior panel of a reinforced concrete slab*, *The Structural Engineer*, **41**, 261–165, 1963.
7. R. PARK and W.R. GAMBLE, *Reinforced concrete slabs*, J. Wiley, New York 1980.

8. A. SAWCZUK and L. WINNICKI, *Plastic behaviour of simply supported concrete plates at moderately large deflections*, Int. J. Solids Struct., **1**, 97–111, 1965.
9. C.R. CALLADINE, *Simple ideas in the large-deflection plastic theory of plates and slabs*, Engineering Plasticity, 93–127, [Eds.] J. Heyman, F.A. Leckie, Cambridge Univ. Press, London 1968.
10. C.T. MORLEY, *Yield-line theory for reinforced concrete slabs at moderately large deflections*, Mag. Concrete Res., **19**, 61, 211–222, 1967.
11. M. JANAS, *Large plastic deformations of reinforced concrete slabs*, Int. J. Solids Struct., **4**, 61–74, 1968.
12. J.R. EYRE, *Direct assessment of safe strength of RC slabs under membrane action*, J. Struct. Engng., ASCE, **123**, 1331–1338, 1997.
13. M. JANAS, *Arching action in elastic-plastic plates*, J. Structural Mechanics, **1**, 277–293, 1973.
14. M. JANAS and J. SOKÓŁ-SUPEL, *Arching action revisited*, Engineering Transactions, **43**, 71–89, 1997.
15. Abaqus, Version 5.4, Hibbitt-Karlsson-Sorensen Inc. 1994.
16. A. RYDZEWSKI and W. ŚIBAK, *Methods for RC plates design following the limit states methodology* (in Polish), Contract Report for the Institute of Fundamental Technological Research, Politechnika Warszawska, Warsaw 1980.

Received January 14, 1999; revised version April 21, 1999.
